Propagation and transformation of upper North Atlantic deep water from the subpolar gyre to 26.5°N

Petit, T. ORCID: https://orcid.org/0000-0002-7922-9363, Lozier, M. S., Rühs, S. ORCID: https://orcid.org/0000-0001-5001-4994, Handmann, P. ORCID: https://orcid.org/0000-0002-5901-4680 and Biastoch, A. ORCID: https://orcid.org/0000-0003-3946-4390 (2023) Propagation and transformation of upper North Atlantic deep water from the subpolar gyre to 26.5°N. Journal of Geophysical Research: Oceans, 128 (8). e2023JC019726. ISSN 2169-9291 doi: 10.1029/2023jc019726 Available at https://centaur.reading.ac.uk/113052/

Propagation and Transformation of upper North Atlantic Deep Water from the subpolar gyre to 26.5°N

T. Petit[1,a], M.S. Lozier[1], S. Rühs[2,b], P. Handmann[2], A. Biastoch[2,3]

[1] School of Earth and Atmospheric Sciences, Georgia Institute of Technology, Atlanta, GA, USA
[2] GEOMAR Helmholtz Centre for Ocean Research Kiel, Kiel, Germany
[3] Kiel University, Kiel, Germany
[a] Present address: National Centre for Atmospheric Science, Department of Meteorology, University of Reading, Reading, UK
[b] Present address: Institute for Marine and Atmospheric research Utrecht, Utrecht University, Netherlands

Key points

- The large majority of uNADW sourced from the Irminger Sea transits through the Labrador Sea before reaching 26.5°N
- Interior pathways along the eastern flank of the Mid-Atlantic Ridge connect the Iceland Basin and Rockall Trough to 26.5°N
- Though uNADW is mainly sourced in the eastern subpolar gyre, its transit in the Labrador Sea is associated with further property changes

Abstract

Because new observations have revealed that the Labrador Sea is not the primary source for waters in the lower limb of the Atlantic Meridional Overturning Circulation (AMOC) during the OSNAP period, it seems timely to re-examine the traditional interpretation of pathways and property variability for the AMOC lower limb from the subpolar gyre to 26.5°N. In order to better understand these connections, Lagrangian experiments were conducted within an eddy-rich ocean model to track upper North Atlantic Deep Water (uNADW), defined by density, between the OSNAP line and 26.5°N as well as within the Labrador Sea. The experiments reveal that 77% of uNADW at 26.5°N is directly advected from the OSNAP West section along the boundary current and interior pathways west of the Mid-Atlantic Ridge. More precisely, the Labrador Sea is a main gateway for uNADW sourced from the Irminger Sea, while particles connecting OSNAP East to 26.5°N are exclusively advected from the Iceland Basin and Rockall Trough along the eastern flank of the Mid-Atlantic Ridge. Although the pathways between OSNAP West and 26.5°N are only associated with a net formation of 1.1 Sv into the uNADW layer, they show large density changes within the layer. Similarly, as the particles transit through the Labrador Sea, they undergo substantial freshening and cooling that contributes to further densification within the uNADW layer.

Plain Language Summary

The North Atlantic Deep Water (NADW) is a cold and fresh water mass formed at high latitudes and advected southward across the North Atlantic as part of the Atlantic Meridional Overturning Circulation (AMOC). The upper part of this water mass (uNADW) has long been considered to be mainly formed in the Labrador Sea. However, new observations have revealed that the Labrador Sea is not the primary source for uNADW, suggesting that the dense water observed at 26.5°N is not necessarily related to Labrador Sea convection. Here, we perform Lagrangian experiments between the subpolar gyre and 26.5°N within an eddy-rich ocean model to show that the Labrador Sea is a main gateway for uNADW sourced from the Irminger Sea and is associated with large property changes within the uNADW layer. Additionally, we reveal direct interior pathways connecting uNADW sourced from the Iceland Basin and Rockall Trough to 26.5°N.

1. Introduction

For decades, the Labrador Sea was thought to be the primary source of deep water formed in the subpolar North Atlantic (McCartney & Talley, 1982; Pickart et al., 2003; Rhein et al., 2002; Straneo et al., 2003; Yashayaev et al., 2007) and carried equatorward via the deep limb of the Atlantic Meridional Overturning Circulation (AMOC). However, observations from the Overturning in the Subpolar North Atlantic Programme (OSNAP) have revealed that dense water formed between the Greenland Scotland Ridge (GSR) and OSNAP East, the latter of which spans a section from the Scottish shelf to the southeast tip of Greenland, contributes far more to the AMOC lower limb than that formed in the Labrador Sea (Lozier et al., 2019).

More precisely, the Irminger and Iceland basins are one of the main sources of dense water formed in the subpolar North Atlantic (Chafik & Rossby, 2019; Petit et al., 2020; Tooth et al., 2022). There, warm and salty water from the subtropical gyre is transformed into cold dense water largely via wintertime convection. Thus, the OSNAP results suggest that the dominant sources for the AMOC lower limb are overflow water transported from the Nordic Seas through the GSR and upper North Atlantic Deep Water (uNADW) formed in the Irminger and Iceland basins. The net formation of deep water through wintertime convection in the Labrador Sea, estimated as the maximum of the overturning stream functions, is seven times smaller than in the eastern subpolar gyre and thus contributes minimally to the mean overturning strength during the OSNAP period (Li et al., 2021b). The interannual variability of the AMOC is also dominated by the eastern

subpolar gyre, such that ventilation in the Labrador Sea is unlikely to play a leading role in the connectivity mechanism between the subpolar and subtropical gyres identified by Kostov et al. (2022) on fast interannual timescales. However, Yeager et al. (2021) uses a long CESM integration to show that deep water formation in the western subpolar gyre dominates the AMOC variability at low frequencies. Two other reasons to highlight the contribution of the Labrador Sea come from recent studies: Freshwater fluxes across OSNAP West are a strong contributor to the total meridional freshwater flux across the entire OSNAP section (Li et al., 2021a) and ventilation of dense water in the Labrador Sea is important for the uptake, storage and export of oxygen in the AMOC lower limb (Koelling et al., 2022).

Because deep water formed in the Labrador Sea was long considered the main source of water for the AMOC lower limb, downstream analyses of AMOC variability have generally been interpreted in terms of Labrador Sea Water (LSW) variability, particularly so at 26.5°N (Frajka-Williams et al. (2016) and Jackson et al. (2016)). Previous studies have interpreted the lag between LSW production and its arrival at 26.5°N as the advective time scale for LSW anomalies to exit the Labrador basin and travel along the Deep Western Boundary Current (DWBC) and interior pathways (Biló & Johns, 2019; Bower et al., 2009). For instance, Van Sebille et al. (2011) and Molinari et al. (1998) estimated a lag of 9-10 years for the LSW salinity anomaly in the Labrador Sea to reach 26.5°N. Curry et al. (1998), who also linked the variability of subtropical temperature at intermediate depths near Bermuda to the variability of convection in the Labrador Sea, yet found a lag of only 6 years. More recently, Chomiak et al. (2022) found longer advection timescales of 10-15 years from a study of both salinity and temperature anomalies of the LSW layer. Importantly, all of these studies implicitly assume that all waters that reach 26.5°N in the LSW density range are primarily sourced by Labrador Sea convection, as opposed to the eastern subpolar North Atlantic. However, given our new understanding of the sources of dense water for the AMOC during the OSNAP period, it seems timely to re-examine the traditional interpretation of pathways and property variability for the AMOC lower limb from the subpolar gyre to 26.5°N.

We posit that there are two possibilities for the pathways of uNADW sourced in the eastern subpolar gyre: 1) the uNADW is mainly advected southward from OSNAP East through various interior pathways, as recently shown for the overflow water (Lozier et al., 2022; Zou et al., 2020b) or 2) a majority of uNADW flows into and out of the Labrador Sea before being exported southward to 26.5°N, along the DWBC and interior pathways.

To connect downstream property variability with source water variability, we aim to assess whether uNADW sourced in the eastern subpolar gyre is further transformed within the uNADW layer once it crosses OSNAP East. Thus, in addition to understanding the pathways of these dense waters we will examine the degree to which the uNADW layer is modified as it moves equatorward and, in particular, as it moves through the Labrador Sea.

In summary, we aim to investigate the mean pathways and along-track property transformation of uNADW between OSNAP East and 26.5°N (Figure 1a) to better connect downstream and upstream deep-water properties. We introduce our Lagrangian experiments in section 2, discuss the experimental results in section 3, investigate uNADW transformation over the Labrador Sea in section 4 and then summarize our results in section 5.

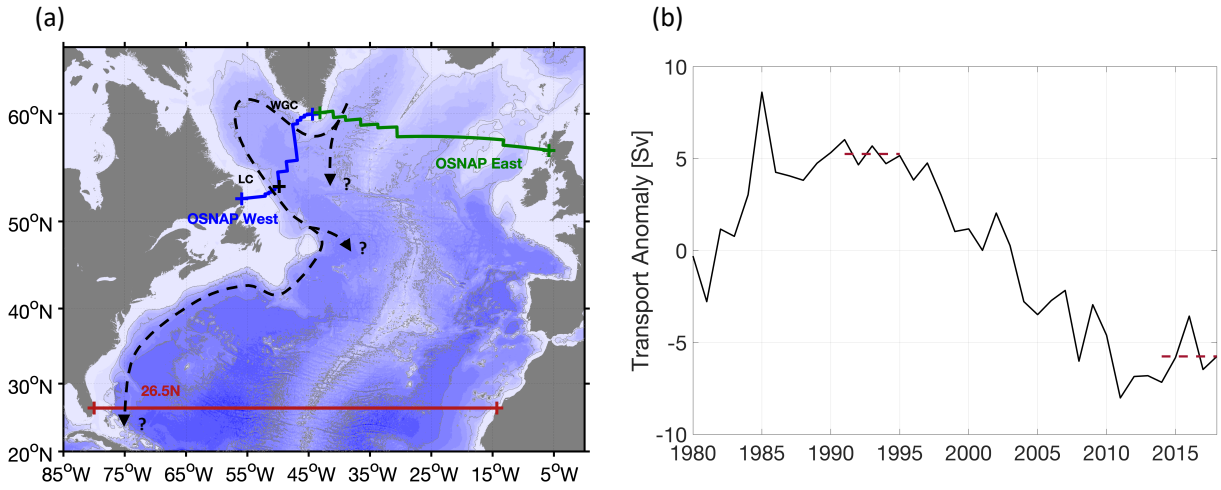

Figure 1. (a) Definition of the sections OSNAP East, OSNAP West and 26.5°N used in the set of experiments EXP_1 in VIKING20X-JRA-short. The sections LC and WGC used for the set of experiments EXP_2 follow the OSNAP West section and are separated by the black cross. The black arrows indicate two possible pathways for uNADW: through the interior or along the boundary via the Labrador Sea. (b) Transport anomaly (Sv) for the uNADW layer as compared to the 1980-2018 mean at the LC section. Dashed red lines indicate the averaged uNADW transport in 1991-1995 and 2014-2018. Positive transports are southward and hence represent export out of the Labrador Sea.

2. Data and Methods

2.1 Observational data from OSNAP and WOCE

Two sets of observations are used to compare the volume transports for the AMOC lower limb between the subpolar gyre and 26.5°N. At subpolar latitudes, we use the monthly estimates of

transports across the OSNAP (Overturning in the Subpolar North Atlantic Program) array from April 2014 to August 2018 (Li et al., 2021b). The gridded (~25×20 km) cross-section transports are estimated from continuous measurements of salinity, temperature and velocity following the International Thermodynamic Equation of Seawater-2010 (TEOS-10, Li et al., 2017). The transport in the AMOC lower limb, defined as water denser than σ_2 = 36.5 kg m^{-3} in Van Sebille et al. (2011), ranges from 15.1 Sv in 2015 to 13.2 Sv in 2017 with an averaged southward transport of 13.9 ± 1 Sv. The uncertainties for transports indicated here and below are estimated as the standard deviation of their interannual variability.

Transports at 26.5°N are analysed from the repeated hydrographic sections of the World Ocean Circulation Experiments (WOCE) at line A05. The A05 section was occupied in summer 1992, 1998, 2004, 2010, 2011 and, more recently, in 2015 (Bryden et al., 2005; Fu et al., 2020). At this section, the transport in the AMOC lower limb ranges from 12.3 Sv in 2004 to 18.2 Sv in 2010 with an average southward transport over all years of 15.9 ± 2 Sv.

2.2 Hindcast simulation of the eddy-rich ocean model configuration, VIKING20X

VIKING20X is an eddy-rich ocean/sea-ice coupled model configuration developed by GEOMAR (Biastoch et al., 2021) and based on the version 3.6 of NEMO ("Nucleus for European Modeling of the Ocean"; Madec & NEMO-team, 2016). It is an updated and expanded version of the well-established VIKING20 configuration that is known for its good representation of the North Atlantic circulation (Böning et al., 2016; Handmann et al., 2018). In VIKING20X, the global horizontal resolution of 1/4° is refined over the full Atlantic Ocean (34°S–70°N) to a horizontal resolution of 1/20°. The vertical resolution is composed of 46 z-levels of 6 m at surface to a maximum of 250 m at depth, with partial bottom cells. The surface boundary conditions were constrained by realistic atmospheric forcing. Biastoch et al. (2021) showed that the choice of the atmospheric forcing dataset is critical for a proper simulation of the AMOC variability. Indeed, the shift from COREv2 forcing (Griffies et al., 2009) to JRA55-do forcing (Tsujino et al., 2020) generally improved the velocity structures of the main currents in the North Atlantic. In this study, we thus use the 5-day mean velocity fields from the nested domain of a hindcast simulation from 1980 to 2018 that uses the JRA55-do forcing. This simulation is referred to as VIKING20X-JRA-short.

2.3 Definition of uNADW in VIKING20X-JRA-short

In the following, we investigate the pathways and hydrographic property evolution of uNADW from OSNAP to 26.5°N as well as around the rim of the Labrador Sea. The layer excludes the overflow water from the Nordic Seas and is defined at σ_2 = 36.5-36.97 kg m^{-3} (approx. σ_0 = 27.65–27.8 kg m^{-3}) in the observations at the Abaco line (Van Sebille et al., 2011) and at OSNAP (Li et al., 2021b). However, this definition needs to be adjusted in VIKING20X-JRA-short to account for a density bias of the model. For a hindcast simulation with VIKING20, Handmann et al. (2018) adjusted the density limits of the uNADW layer to σ_2 = 36.68-37.03 kg m^{-3} in the central Labrador Sea. The upper limit is associated with the density of the maximum overturning at the OSNAP line in the model. The lower limit has been estimated by identifying the isopycnal with the lowest statistical depth variation. We use the same density limits to define the uNADW layer in VIKING20X-JRA-short because of a similar bias in density between the two models (not shown).

We use the terms "source" and "net formation" independently throughout our analysis to refer to the production of water into the uNADW layer, as defined by the density range σ_2 = 36.68–37.03 kg m^{-3}, without considering specific classes of uNADW. We use the term "transformation" to refer to changes in hydrographic properties within the uNADW layer. Note that our experiments do not allow us to determine the specific mechanisms responsible for these net formations or transformations, which can be forced by air-sea interaction and/or by interior mixing.

Because the uNADW density at the exit of the subpolar gyre is highly variable in time (Yashayaev & Loder, 2016), we compare the uNADW properties of 2 specific periods (1991-1995 and 2014-2018; see section 2.4) within the isopycnals that bound the core of uNADW from 1980-2018 across the Labrador Current (LC) section. To identify these bounding isopycnals we compute the standard deviation of the density associated with the maximum transport at the LC section during this period. Hence, the core of uNADW is defined by the density range 36.87-37.0 kg m^{-3} in VIKING20X-JRA-short.

2.4 Lagrangian experiments with ARIANE

We use the software ARIANE (version 2.3) to perform two sets of Lagrangian experiments (Blanke & Raynaud, 1997; van Sebille et al., 2018). ARIANE computes particle trajectories in a time-varying three-dimensional velocity field. The particle trajectories can be interpreted as stream

tubes, allowing for the estimation of volume transports between the release and destination sections (e.g., van Sebille et al. 2018). The release section defines the starting point for the stream tubes, where the number of particles seeded by ARIANE is proportional to the transport field and can be restricted to a density layer. The evolution of the particle density along these trajectories is estimated by linearly interpolating the temperature and salinity fields at each position of the particle between neighbouring grid points. At the destination section, the volume flux of all particles arriving in a specific density bin are then summed to yield the total volume transport. In these experiments, the integration of the particle trajectories stops once the particle reaches a predefined destination section or once the maximum integration time is reached.

A first set of experiments, called EXP_1, is designed to track particles of uNADW from 26.5°N back to the OSNAP sections, determine whether they are sourced from OSNAP East or OSNAP West, and record the along-track evolution of their hydrographic properties between the sections (Figure 1a). In EXP_1, we perform 10 individual experiments where particles are released in the uNADW layer at 26.5°N (from coast to coast) every 5 days during every year of the 2009 to 2018 period. These particles are then advected backward in time until they reach one of the destination sections, OSNAP East or OSNAP West, over the integration period. We use a maximum integration time of 78 years in order to have less than ~13% of particles 'lost' between the release and destination sections. To achieve this integration time, we loop twice through the velocity field of the 1980-2018 period. Although a loop can introduce unrealistic jumps in the evolution of the hydrographic properties (Döös et al., 2008; Thomas et al., 2015), the error in the along-track property of the particles is negligible in this analysis due to the high number of particles seeded (i.e., $O(10^5)$ per experiment) and to the small drift in temperature and salinity observed in the model during this period (i.e., trends of -0.0014°C and -0.0114 psu over the nest and for the entire water column). Moreover, Figure S1 shows that the density changes at the looping point for the particles seeded in EXP_1 are small in comparison to their density changes between the release and destination sections.

The second set of experiments, called EXP_2, is designed to back track particles of uNADW from the LC section to the West Greenland Current (WGC) section and analyse the evolution of their hydrographic properties within the Labrador Sea (Figure 1a). In EXP_2, we release particles in the uNADW layer at the LC section every 5 days during every year of the OSNAP period (2014-

2018). The particles are then advected backward in time until they reach the WGC section in a maximum of 5 years. A maximum integration time of 5 years is sufficient because only 1% of the particles remain in the Labrador Sea after 5 years of integration. However, as the OSNAP period is associated with a relatively weak uNADW export through the LC section (Figure 1b), the EXP_2 is additionally performed over the period 1991-1995, which exhibits a relatively strong uNADW export. Note that the particles considered in EXP_2 are not a subset of the particles released of EXP_1 because of the difference in the time periods considered.

2.5 Model evaluation: Eulerian transformation of uNADW

Biastoch et al. (2021) showed that the large-scale horizontal circulation of the North Atlantic, the deep water transport in the boundary current, as well as the mean structure and variability of the AMOC are well simulated in VIKING20X-JRA-short as compared to observations. For instance, a major part of the overturning occurs at OSNAP East instead of OSNAP West in the model, which is consistent with OSNAP observations. A good representation of the convective processes in the subpolar North Atlantic, including the shift of the convection from the Labrador to the Irminger Sea in 2015–2018, was also highlighted by Rühs et al. (2021).

In this section, we further show that the uNADW transport at OSNAP and 26.5°N is well reproduced in the model. Indeed, Figure 2 shows the transport estimated per density bin of 0.01 kg m^{-3} at these two sections in both model and observations. The observational transports at OSNAP are averaged over the OSNAP period and those at the A05 section are an average of the 3 occupations in the 2010s. Using the full temporal record of VIKING20X-JRA-short, we estimate that the bias introduced by the truncated observational time periods at the two sections is ~ 0.39 Sv in the uNADW layer.

Overall, the structure of the transports across OSNAP and 26.5°N is consistent between the model and observations. The difference in transport between these two sections allows us to identify the transformation associated within each density bin, although it does not allow for a determination of the specific mechanism (e.g., buoyancy forcing and interior mixing) that create this transformation. The transformation between the sections shows a net increase in transport for subpolar mode water between 36.1-36.4 kg m^{-3} and a net decrease in transport for overflow water denser than 37.0 kg m^{-3} (Figures 2c, f). Though the transformation over the uNADW layer is highly

variable in density, there is a net increase of 3.1 Sv in the observations and of 4.0 Sv in VIKING20X-JRA-short, which is mainly localized in the lower part of the layer. Because the volume budget in the uNADW layer is remarkably consistent between the model and observations, we are confident in the use of VIKING20X-JRA-short for our investigation of the uNADW pathways between these sections.

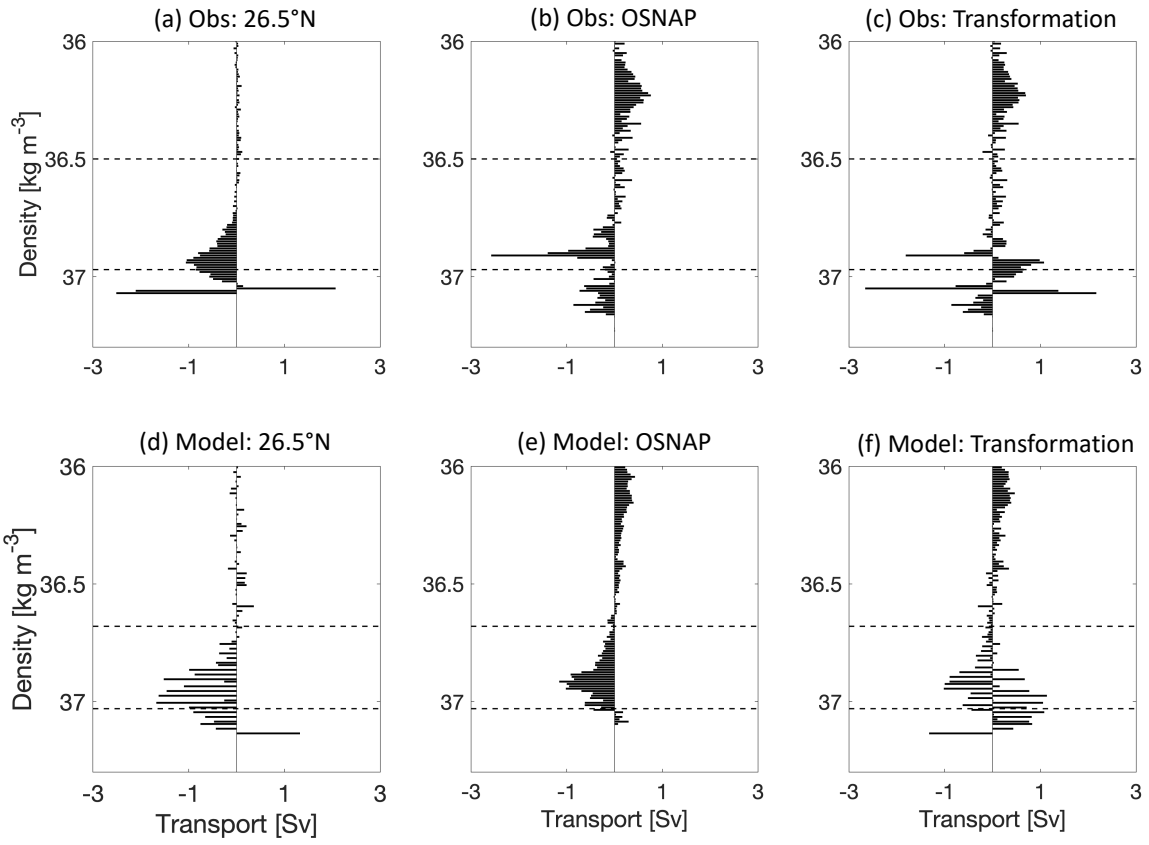

Figure 2. (a-c) Observed and (d-f) simulated transports (Sv) integrated in density bins of 0.01 kg m^{-3} at 26.5°N and OSNAP. Dashed lines indicate the potential density for the uNADW layer, with subpolar mode water and overflow waters residing above and below this layer, respectively. In observations, the transports at OSNAP are averaged during the 4 years of observations, while the transports at 26.5°N include the A05 sections in 2010, 2011 and 2015. Positive transports are northward. (c,f) Difference in transport between 26.5°N and OSNAP. Positive (negative) transformation is associated with net increase (decrease) of transport in the respective density bin between the two sections.

3. Source and transformation of uNADW from OSNAP to 26.5°N

The pathways and net property evolution of uNADW observed at 26.5°N are analyzed with the Lagrangian experiments EXP_1. At the release section, the particles seeded in the uNADW layer are mainly localized along the western boundary of the section (52.5-53.5°W) and associated with

a relatively strong transport for densities > 36.85 kg m^{-3} (Figure S2). After accounting for the ~55 Sv of particles that recirculate southward across the release section, we track a total of 16.1 Sv of particles to their destination over the integration time period. The upstream distribution of these particles (Figure 3a) reveals that they are largely advected from OSNAP West (12.4 Sv or 77%), mainly along the western boundary of the section (Figure S2c), rather than from OSNAP East (0.7 Sv or 4.6%). The interannual variability of the transport at 26.5°N (Figure 3b) is also dominated by the OSNAP West contributions. As for other sources, 1.8 Sv does not reach a section during the integration time and is considered "lost" in the study area, mainly east of the Mid-Atlantic Ridge (not shown), and 1.2 Sv recirculates across the release section in an adjoining density layer. Therefore, the main source for uNADW at 26.5°N is OSNAP West, which suggests that uNADW sourced from the eastern subpolar gyre is mainly advected through the Labrador Sea instead of being directly advected from OSNAP East through interior pathways.

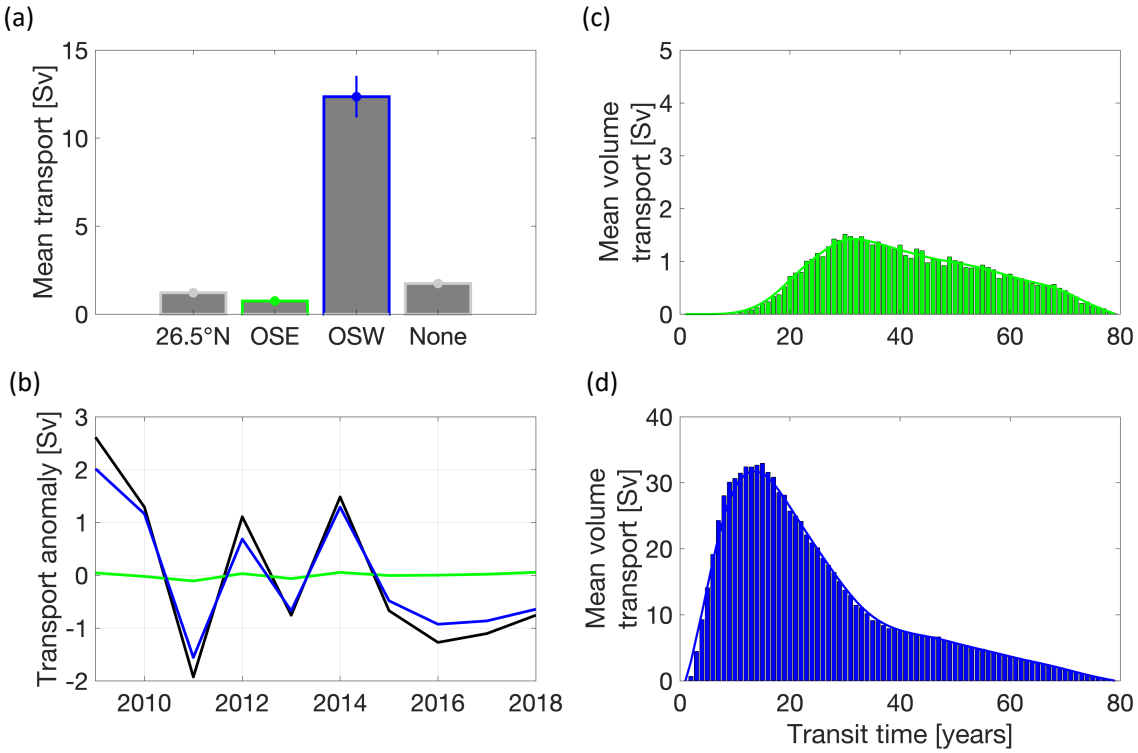

Figure 3. Sources for uNADW deduced from the set of experiments EXP_1. (a) Mean volumetric contributions of the individual sources to uNADW at 26.5°N. Dots and lines indicate the mean and standard deviation of the transport over the 10 experiments, respectively. (b) Interannual variability of the total uNADW transport anomaly (black) and its individual contributions OSNAP East (OSE in green) and OSNAP West (OSW in blue) estimated with the 10 different release years. (c-d) Transit times for the particles to reach 26.5°N from the destination sections (c) OSNAP East and (d) OSNAP West. Bars indicate the mean transit time distributions for the set of 10 experiments and the lines indicate the distribution smoothed using a 5-points moving average.

The transit times of the particles advected from OSNAP West show that more than 50% reach 26.5°N in 20 years, with the highest number of particles (modal value) reaching the section after 14 years (Figure 3d). The advective transit time of the particles from OSNAP East is twice larger than from OSNAP West. Indeed, the majority of particles from OSNAP East reach 26.5°N in 40 years with the highest number of particles reaching the section after 31 years (Figure 3c). The difference in advective transit time between the two source sections is time invariant and is explained by different uNADW pathways.

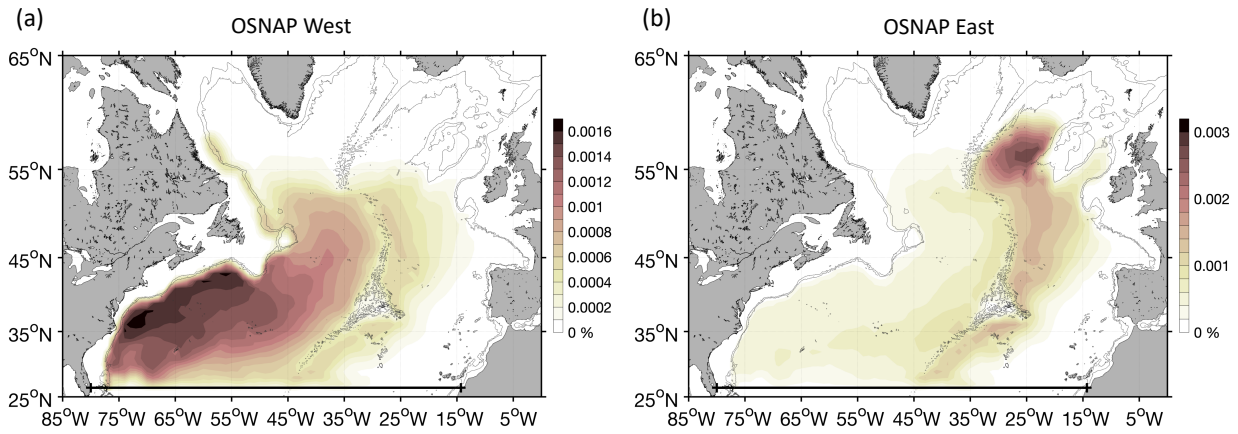

Figure 4. Dominant uNADW pathways between OSNAP and 26.5°N, from EXP_1 for particle subsets reaching (a) OSNAP West and (b) OSNAP East. The probability that a certain section is crossed by a particle during its transit is estimated as the percentage of particle counts for each bin of a (0.5° x 0.5°) grid during the 2 cycles of the experiment, such that the probabilities of all bins sum to 100%. Repeat crossings of a single particle are included in the counts. The 10 individual probability distributions of each experiment in EXP_1 are then averaged. The black line shows the release section at 26.5°N.

The uNADW pathways between 26.5°N and OSNAP West, shown as a probability density distribution in Figure 4a, reveal a myriad of pathways, including those in boundary current and in the interior, consistent with past observational and modelling studies (Bower et al., 2009 and Lozier et al. 2013). Nevertheless, the majority of the particles remain west of the Mid-Atlantic Ridge instead of crossing the ridge eastward. On the contrary, the uNADW pathways between 26.5°N and OSNAP East are mainly restricted to the eastern side of the Mid-Atlantic Ridge (Figure 4b). The small fraction of particles that cross the ridge westward through deep fracture zones (e.g. the Charlie Gibbs Fracture Zone and other deep fractures further south) preferentially follow its western flank rather than the western boundary current. Therefore, the Mid-Atlantic Ridge acts as a barrier in the propagation of uNADW, such that the particles exiting the eastern subpolar gyre

mainly propagate along its eastern flank, while those exiting the western subpolar gyre mainly propagate to the west of the ridge.

Moreover, all particles coming from OSNAP East leave the eastern subpolar gyre through the Iceland Basin and Rockall Trough instead of the Irminger Sea. Hence, uNADW sourced from the Irminger Sea is not directly advected southward via interior pathways but is instead advected westward through the Labrador Sea. These results are consistent with a recent study that details the different Lagrangian pathways of the overflow waters from the Irminger and Labrador basin compared to the Iceland basin (Lozier et al., 2022).

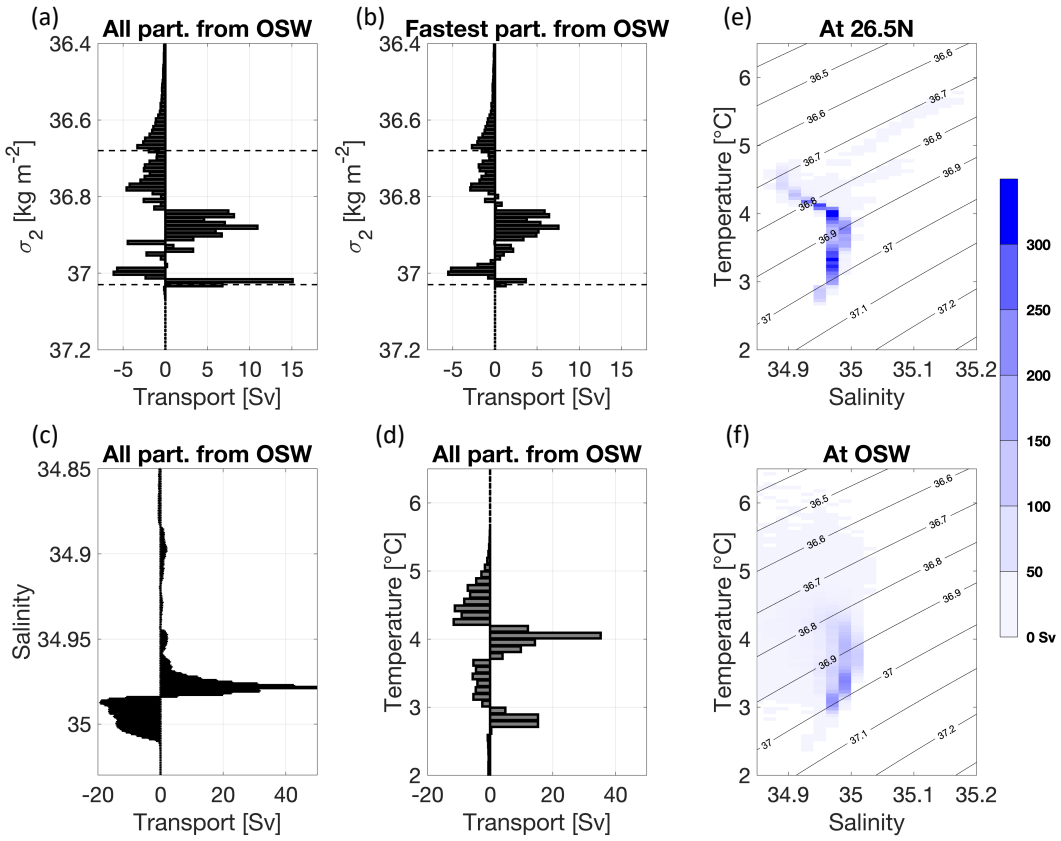

Figure 5. Thermohaline properties of uNADW reaching OSNAP West from the set of experiments EXP_1. (a-d) Difference in mean volume transport between the release section 26.5°N and the destination section OSNAP West. The volume transport is estimated per (a-b) density bins of 0.01 kg m^{-3}, (c) salinity bins of 0.001 and (d) temperature bins of 0.1°C. Panel (d) includes only the 50% fastest particles reaching OSNAP West. Positive (negative) transformation is associated with net increase (decrease) of transport in the respective density bin from OSNAP West to 26.5°N. Dashed lines indicate the potential density σ_2 = 36.68 and 37.03 kg m^{-3} for the uNADW layers in VINKING20X. (e-f) Volume transport (Sv) in each temperature and salinity bin at (e) the release section and the (f) destination section.

The property transformation of uNADW is now analyzed for particles advected between OSNAP West and 26.5°N. With our convention, a positive (negative) transformation is associated with net increase (decrease) of transport in the respective density range from OSNAP West to 26.5°N. A net increase of only 1.1 Sv is found in the uNADW layer between the sections, such that 96.9 ± 0.4 % of the particles belong to the uNADW density range at both the release and destination sections. However, there are large density changes within the uNADW layer (Figure 5a). In particular, we note a net increase in uNADW transport between 36.84 to 36.91 kg m^{-3} and at 37.02 kg m^{-3}, and a net decrease in uNADW transport between 36.91 to 37.02 kg m^{-3} and at $\sigma_2 < 36.84$ kg m^{-3}. The uNADW densification is associated with a freshening from ~35 to ~34.98 and a cooling from ~4.5°C to ~4°C and at ~2.8°C (Figures 5 c-d). The temperature/salinity diagrams at the two sections in Figures 5 (e-f) confirm that these transformations in salinity and temperature are mainly localized within the uNADW layer.

By comparing these transformations with those estimated for a subclass of particles, we find that the transformations in the density range of 36.68-36.91 kg m^{-3} are mainly attributed to the 50% fastest particles (Figure 5b). Considering that these fast particles preferentially follow the boundary current, the transformation is possibly explained by the relatively strong gradient between the boundary current and the interior. However, the net increase in uNADW transport at 37.02 kg m^{-3} is mainly attributed to particles remaining in the basin for more than 20 years, implying that particles reaching 26.5°N in more than 20 years play a role in the transformation of only the very dense uNADW.

4. Transformation of uNADW in the Labrador Sea

Since the Labrador Sea is a key pathway for uNADW formed over the eastern subpolar gyre, we now investigate whether uNADW is further modified as it passes through the Labrador Sea. We first use the EXP_2 performed during 2014-2018. In this set of experiments, nearly all the particles released at the LC section are advected from the WGC section, and more than 60% of the particles reach the destination section after only 1 year. This time scale is consistent with previous studies that document a transit time along the boundary current of the Labrador Sea of 1-2 years (Bower et al., 2009; Feucher et al., 2019; Georgiou et al., 2020) and with Lagrangian experiments that tracked backward in time overflow water from the Denmark Strait to 53°N in VIKING20X-JRA-OMIP (Fröhle et al., 2022).

During its transit through the Labrador Sea, the uNADW largely follows the boundary current in the basin (Figure 6a). This pathway is particularly clear for particles reaching the destination section in less than 1 year (Figure 6c). On the contrary, the particles reaching the destination section in more than 4 years recirculate in the interior of the basin (Figure 6d). This area is associated with deep mixed layer depths during wintertime, which were relatively deeper in the 90s than during the OSNAP period (Rühs et al., 2021).

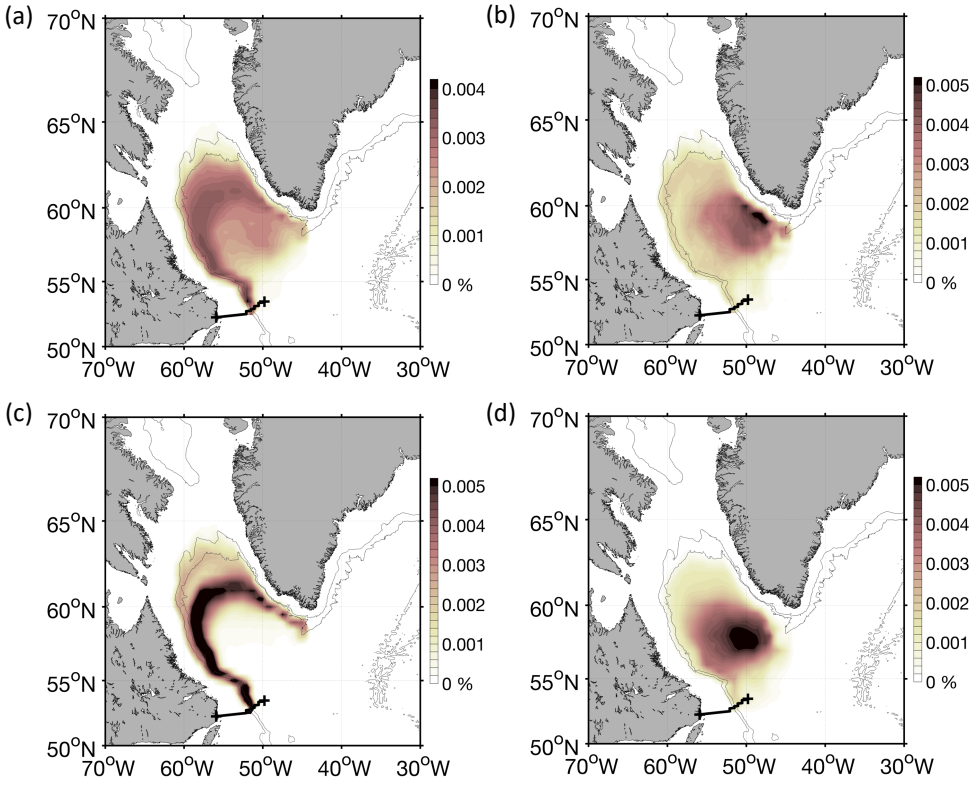

Figure 6. Probability distribution from EXP_2 performed during 2014-2018 for (a) all the particles released at the LC and for 3 subclasses of the experiment: (b) particles with a densification higher than 0.1 kg m^{-3} between the release and destination sections, (c) particles reaching the destination section in less than 1 year, (d) particles reaching the destination section in more than 4 years. The 4 individual probability distributions are estimated as described in Figure 4 and are then averaged together. The black line shows the release section at the LC. Bathymetry is contoured at 1000 m and 2000 m.

The difference in the density, salinity and temperature transformation along these pathways between the 5-year period of relatively strong (1991-1995) and the 5-year period of relatively weak (2014-2018) uNADW export is next examined. During the 2014-2018 period, 31.7% of subpolar mode water is transformed into uNADW over the Labrador Sea (Figure 7a). During the 1991-1995 period, only 21.0% is transformed (Figure 7d). For both time periods, the boundary-following

particles that are in the Labrador Sea for less than one year account for most of the transformation (Figures S3 and 6c). The difference in the proportion of subpolar mode water transformed into uNADW (e.g. which is equivalent to the net volume of uNADW production as compared to the outflowing volume of uNADW across OSNAP West) between the 2 periods is explained by the vertical density structure of the inflowing water. The inflowing water is evenly distributed between the subpolar mode water and uNADW layers in 1991-1995, while it is mainly localized in the subpolar mode water layer in 2014-2018. Thus, the strong buoyancy loss over the Labrador Sea during the 1991-1995 period contributes to both the net volume of newly formed uNADW and to further densification of uNADW within the layer.

However, although the net increase in uNADW transport is small during these 2 periods, the particles undergo substantial freshening and cooling between the WGC and LC sections. In particular, we note a cooling of water from ~4-6°C to ~3-4°C (Figures 7c, f) and a freshening in salinity from ~34.99-35.1 to ~34.97 (Figures 7b, e). These transformations are larger during the strong convection period of the 90s than during the OSNAP period.

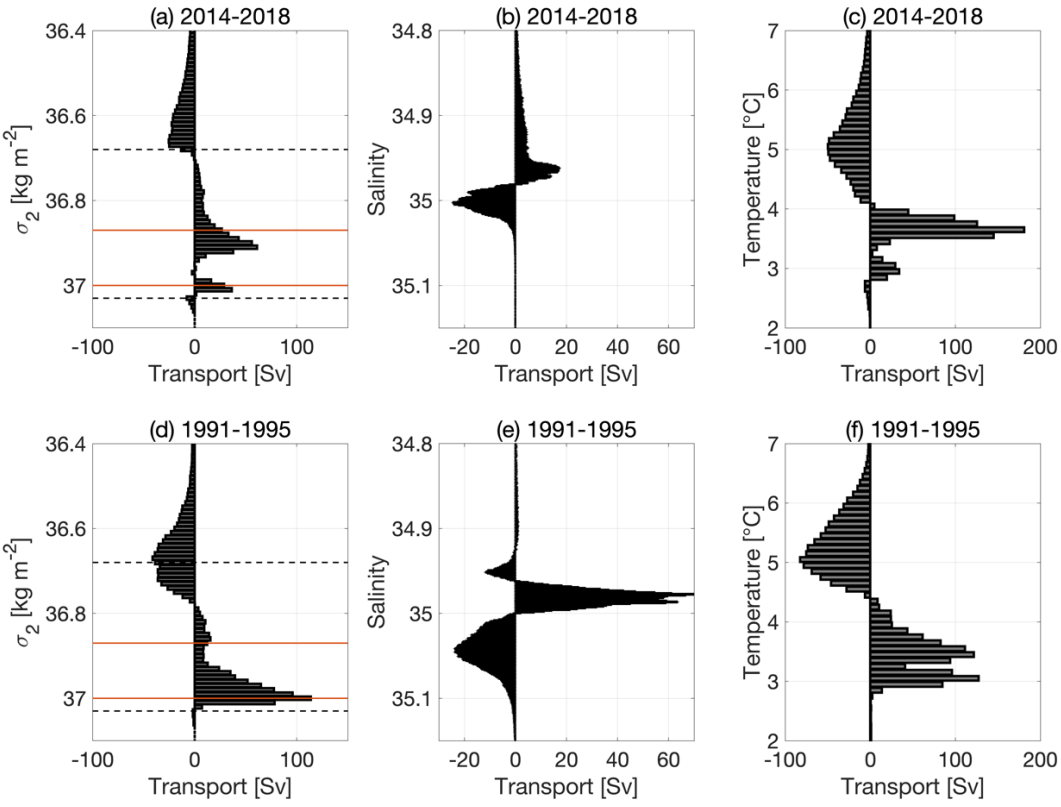

Figure 7. Difference in mean volume transport between the release section LC and the destination section WGC from the set of experiments EXP_2 performed during (a-c) 2014-2018 and (d-f) 1991-1995. The volume transport is estimated per (a, d) density bins of 0.01 kg m^{-3}, (b, e) salinity bins of 0.001 psu and (c, f) temperature bins of 0.1°C. Positive transformation is associated with a net increase of transport in the respective density bin over the Labrador Sea. Dashed lines indicate the potential density σ_2 = 36.68 and 37.03 kg m^{-3} for the uNADW layers in VINKING20X. Red lines indicate the limits in density for the uNADW core in the LC specifically.

Consequently, Figures 7a and 7d show that the uNADW formed in 1991-1995 (with a density peak at ~37 kg m^{-3}) spans the densest part of the averaged core of uNADW, as identified by the red lines, while the uNADW formed in 2014-2018 (with a density peak at ~36.91 kg m^{-3}) spans its lightest part. Most of this transformation occurs within the uNADW layer to particles remaining in the center of the Labrador Sea for more than 1 year (Figures S3 and 6d). In agreement with previous studies (Jackson et al., 2016; Yashayaev & Loder, 2016), we thus show that the uNADW transformed in the Labrador Sea is denser in the 90s than during the OSNAP period. Therefore, the strength of the convection in the Labrador Sea influences the changes in uNADW properties within the AMOC lower limb.

Finally, we show that the largest density changes (greater than 0.1 kg m^{-3} in Figure 6b) are mainly localized along the West Greenland Current between Eirik Ridge and Cape Desolation, which is where the Irminger Rings are shed and recirculation takes place (Cuny et al., 2002), instead of the interior of the basin. This agrees well with previous studies revealing the importance of density changes along the boundary current for the dynamic of the subpolar gyre (Menary et al., 2020; Spall, 2004; Straneo, 2006), as well as with a recent study (Fröhle et al., 2022) showing that uNADW formation in the Labrador Sea on decadal time scales is mainly a result of diapycnal mass fluxes over this area rather than by mixed layer formation over the interior of the basin.

To summarize, the Labrador Sea is not associated with large uNADW formation, but is a key pathway for uNADW sourced over the eastern subpolar gyre and is a key location for uNADW densification within the AMOC lower limb.

5. Conclusion and discussion

In this study, the mean pathways and along-stream transformation of uNADW from OSNAP to 26.5°N are investigated using Lagrangian experiments performed in a hindcast simulation with the eddy-rich ocean model VIKING20X-JRA-short. In order to better understand the sources of transport and density anomalies of uNADW that are observed at 26.5°N, particles were released

at 26.5°N and advected backward in time until they reached the OSNAP East or OSNAP West sections. In this first set of experiments, we show that OSNAP West is the main source section for uNADW (77%), and that a large majority of uNADW at 26.5°N trace back from the Labrador Sea instead of being directly advected from OSNAP East through interior pathways.

In particular, we show that all the particles advected southward from OSNAP East without a detour in the Labrador Sea leave the eastern subpolar gyre from the Iceland Basin and Rockall Trough rather than from the Irminger Sea. The Labrador Sea is thus the main gateway for uNADW from the Irminger Sea to the subtropical latitudes. This advective pathway compares well with the observed propagation pathways of the underlying overflow water shown by Lozier et al. (2022), where 94% of their floats enter the Labrador Sea despite the sharply curved Eirik Ridge.

Although only a small volume of uNADW is directly advected from OSNAP East to 26.5°N, we further show that the particles from the Iceland Basin and Rockall Trough do not follow the boundary current but propagate southward along the eastern flank of the Mid-Atlantic Ridge. This southward pathway is consistent with the observed spread of overflow water from the Iceland Basin (Lozier et al., 2022) and has been estimated to contribute to 38 ± 14 % of the whole basin meridional transport from 50°N to 35°N (Zhai et al., 2021). Its propagation is possibly explained by the mesoscale activity of the North Atlantic Current at the entrance of the basin, which is known to divert deep water eastward at the Charlie-Gibbs Fracture Zone (Zou et al., 2020b).

On the contrary, the particles reaching 26.5°N from OSNAP West follow both the boundary current and interior pathways west of the Mid-Atlantic Ridge. The distribution of the interior pathways agrees well with the observed LSW pathways from Argo floats shown by Biló & Johns (2019), and can partially delay the propagation of uNADW anomalies between the sections (Chomiak et al., 2022). The uNADW anomalies are, indeed, commonly used to infer advective timescales between the Labrador Sea and 26.5°N. However, we show that the uNADW exported from the Labrador Sea is modified along these pathways. Indeed, although the transport in the uNADW layer increases by only 1.1 Sv between OSNAP West and 26.5°N, we highlight that these pathways are associated with large temperature and salinity changes within the uNADW layer. The mechanism of transformation between the subpolar and subtropical gyres could be due to entrainment of dense water between the boundary current and/or the interior or by mixing with surrounding water during recirculation within the subpolar gyre. Further investigation, however,

is needed to reveal the relative importance of these different densification processes and of their temporal variability.

During the transit through the Labrador Sea, the second set of experiments shows only a small increase of transport in the uNADW layer, which is slightly more pronounced in 2014-2018 (31.7%) than in 1991-1995 (21.0%). However, although the uNADW formation is small during these 2 periods, we show that strong convection years (1991-1995) lead to large changes in salinity and temperature that drive uNADW densification within the AMOC lower limb. This is consistent with the density compensated overturning shown by Zou et al. (2020a) in the Labrador Sea. Thus, the buoyancy loss over the Labrador Sea contributes to both the net volume of newly formed uNADW for particles remaining less than 1 year in the basin and to a further densification of uNADW within the layer for particles remaining more than 1 year in the basin. These two (indirect and direct) routes and the associated difference in residence time scale are consistent with Georgiou et al. (2021) which showed that the indirect route governs the transformation within the denser layers.

In addition, it has been shown that the circulation of the subpolar gyre can be influenced by changes in the dynamics of the boundary current. An increase in the interior deep convection of the Labrador Sea would lead to an increase in the radial density gradient and, thus, to a stronger baroclinic flow along the boundary current (Straneo, 2006; Born & Stocker, 2014; Ghosh et al., 2023).

These two mechanisms imply that, although Labrador Sea convection is not the primary source for the lower limb of the AMOC, the strength of convection in the Labrador Sea could influence the AMOC by modifying the properties of the uNADW that propagates downstream to 26.5°N and, possibly, the uNADW that flows from the Labrador Sea to the eastern subpolar gyre via recirculation pathways. This is consistent with previous studies showing that eastward recirculation is important for setting the hydrography of the eastern subpolar gyre at both interannual (Asbjørnsen et al., 2021; Fox et al., 2022; Holliday et al., 2020) and decadal timescales (Yeager et al., 2021). The impact of these modified uNADW properties for the AMOC through recirculation in the subpolar gyre is beyond the scope of our analysis and is the purpose of a follow-up study.

Acknowledgements

T.P. and M.S.L. acknowledge support from the National Science Foundation Physical Oceanography Program (NSF OCE-1948335). T.P. was also funded by the NERC SNAP-DRAGON project (NE/T013494/1). For the purpose of open access, the author has applied a 'Creative Commons Attribution (CC BY)' licence to any Author Accepted Manuscript version arising.

Open Research

The OSNAP data used for this work are available online at https://www.o-snap.org/observations/data/ (Fu et al, 2023a) (Fu et al, 2023b).

References

Asbjørnsen, H., Johnson, H. L., & Arthun, M. (2021). Variable Nordic Seas Inflow Linked to Shifts in North Atlantic Circulation. *Journal of Climate*, *34*(17), 7057–7071. https://doi.org/10.1175/JCLI-D-20-0917.1

Biastoch, A., Schwarzkopf, F. U., Getzlaff, K., Rühs, S., Martin, T., Scheinert, M., et al. (2021). Regional imprints of changes in the Atlantic Meridional Overturning Circulation in the eddy-rich ocean model VIKING20X. *Ocean Science*, *17*(5), 1177–1211. https://doi.org/10.5194/os-17-1177-2021

Biló, T. C., & Johns, W. E. (2019). Interior Pathways of Labrador Sea Water in the North Atlantic From the Argo Perspective. *Geophysical Research Letters*, *46*(6), 3340–3348. https://doi.org/10.1029/2018GL081439

Blanke, B., & Raynaud, S. (1997). Kinematics of the Pacific Equatorial Undercurrent: An Eulerian and Lagrangian approach from GCM results. *Journal of Physical Oceanography*, *27*(6), 1038–1053. https://doi.org/10.1175/1520-0485(1997)027<1038:KOTPEU>2.0.CO;2

Böning, C. W., Behrens, E., Biastoch, A., Getzlaff, K., & Bamber, J. L. (2016). Emerging impact of Greenland meltwater on deepwater formation in the North Atlantic Ocean. *Nature Geoscience*, *9*(7), 523–527. https://doi.org/10.1038/ngeo2740

Born, A., and T. F. Stocker, 2014: Two Stable Equilibria of the Atlantic Subpolar Gyre. *J. Phys. Oceanogr.*, **44**, 246–264, https://doi.org/10.1175/JPO-D-13-073.1

Bower, A. S., Lozier, M. S., Gary, S. F., & Böning, C. W. (2009). Interior pathways of the North Atlantic meridional overturning circulation. *Nature*, *459*(7244), 243–247. https://doi.org/10.1038/nature07979

Bryden, H. L., Longworth, H. R., & Cunningham, S. A. (2005). Slowing of the Atlantic meridional overturning circulation at 25° N. *Nature*, *438*(7068), 655–657. https://doi.org/10.1038/nature04385

Chafik, L., & Rossby, T. (2019). Volume, Heat, and Freshwater Divergences in the Subpolar North Atlantic Suggest the Nordic Seas as Key to the State of the Meridional Overturning Circulation. *Geophysical Research Letters*, *46*(9), 4799–4808. https://doi.org/10.1029/2019GL082110

Chomiak, L. N., Yashayaev, I., Volkov, D. L., & Schmid, C. (2022). Inferring Advective Timescales and Overturning Pathways of the Deep Western Boundary Current in the North Atlantic Through Labrador Sea Water Advection Journal of Geophysical Research : Oceans,

1–23. https://doi.org/10.1029/2022JC018892
Cuny, J., Rhines, P. B., Niiler, P. P., & Bacon, S. (2002). Labrador Sea Boundary Currents and the Fate of the Irminger Sea Water. *Journal of Physical Oceanography*, *32*(2), 627–647. https://doi.org/10.1175/1520-0485(2002)032%3C0627:lsbcat%3E2.0.co;2
Curry, R. G., McCartney, M. S., & Joyce, T. M. (1998). Linking subtropical deep water climate signals to North Atlantic subpolar convection variability. *Nature*, *391*, 575−577.
Döös, K., Nycander, J., & Coward, A. C. (2008). Lagrangian decomposition of the Deacon Cell. *Journal of Geophysical Research*, *113*(C7), C07028. https://doi.org/10.1029/2007JC004351
Feucher, C., Garcia-Quintana, Y., Yashayaev, I., Hu, X., & Myers, P. G. (2019). Labrador Sea Water Formation Rate and Its Impact on the Local Meridional Overturning Circulation. *Journal of Geophysical Research: Oceans*, *124*(8), 5654–5670. https://doi.org/10.1029/2019JC015065
Fox, A. D., Handmann, P., Schmidt, C., Fraser, N., Rühs, S., Sanchez-Franks, A., et al. (2022). Exceptional freshening and cooling in the eastern subpolar North Atlantic caused by reduced Labrador Sea surface heat loss. *Ocean Science*, 18, 1507–1533, https://doi.org/10.5194/os-18-1507-2022
Fröhle, J., Handmann, P. V. K., Biastoch, A., & Kiel, C. (2022). Major sources of North Atlantic Deep Water in the subpolar North Atlantic from Lagrangian analyses in a high – resolution ocean model, (May), 1–33. Retrieved from https://doi.org/10.5194/egusphere-2022-313
Fu, Y., Lozier, M. S., Biló, T.C., Bower, A., Cunningham, S., Cyr, F., et al. (2023a). Meridional Overturning Circulation Observed by the Overturning in the Subpolar North Atlantic Program (OSNAP) Array from August 2014 to June 2020 [Dataset]. *Georgia Institute of Technology*. http://doi.org/10.35090/GATECH/70342
Fu, Y., Lozier, M.S., Biló, T.C. et al. Seasonality of the Meridional Overturning Circulation in the subpolar North Atlantic. *Commun Earth Environ 4*, 181 (2023b). https://doi.org/10.1038/s43247-023-00848-9
Fu, Y., Feili, L., Karstensen, J., & Wang, C. (2020). A stable Atlantic Meridional Overturning Circulation in a changing North Atlantic Ocean since the 1990s. *Science Advances*, *6*(48). https://doi.org/10.1126/sciadv.abc7836
Georgiou, S., Ypma, S. L., Brüggemann, N., Sayol, J-M., van der Boog, C. G., Spence, P., et al. (2021). Direct and indirect pathways of convected water masses and their impacts on the overturning dynamics of the Labrador Sea. *Journal of Geophysical Research: Oceans*, 126, e2020JC016654. https:// doi.org/10.1029/2020JC016654
Georgiou, S., Ypma, S. L., Brüggemann, N., Sayol, J. M., Pietrzak, J. D., & Katsman, C. A. (2020). Pathways of the water masses exiting the Labrador Sea: The importance of boundary–interior exchanges. *Ocean Modelling*, *150*(November 2019), 101623. https://doi.org/10.1016/j.ocemod.2020.101623
Ghosh, R., and Coauthors, 2023: Two Distinct Phases of North Atlantic Eastern Subpolar Gyre and Warming Hole Evolution under Global Warming. *J. Climate*, 36, 1881–1894, https://doi.org/10.1175/JCLI-D-22-0222.1
Griffies, S. M., Biastoch, A., Böning, C., Bryan, F., Danabasoglu, G., Chassignet, E. P., et al. (2009). Coordinated Ocean-ice Reference Experiments (COREs). *Ocean Modelling*, *26*(1–2), 1–46. https://doi.org/10.1016/j.ocemod.2008.08.007
Handmann, P., Fischer, J., Visbeck, M., Karstensen, J., Biastoch, A., Böning, C., & Patara, L. (2018). The Deep Western Boundary Current in the Labrador Sea From Observations and a High-Resolution Model. *Journal of Geophysical Research: Oceans*, *123*(4), 2829–2850.

https://doi.org/10.1002/2017JC013702
Holliday, N. P., Bersch, M., Berx, B., Chafik, L., Cunningham, S., Florindo-López, C., et al. (2020). Ocean circulation causes the largest freshening event for 120 years in eastern subpolar North Atlantic. *Nature Communications*, *11*(1), 585. https://doi.org/10.1038/s41467-020-14474-y
Jackson, L. C., Peterson, K. A., Roberts, C. D., & Wood, R. A. (2016). Recent slowing of Atlantic overturning circulation as a recovery from earlier strengthening. *Nature Geoscience*, *9*(7), 518–522. https://doi.org/10.1038/ngeo2715
Koelling, J., Atamanchuk, D., Karstensen, J., Handmann, P., & Wallace, D. W. R. (2022). Oxygen export to the deep ocean following Labrador Sea Water formation. *Biogeosciences*, *19*(2), 437–454. https://doi.org/10.5194/bg-19-437-2022
Kostov, Y., Messias, M.-J., Mercier, H., Johnson, H. L., & Marshall, D. P. (2022). Fast mechanisms linking the Labrador Sea with subtropical Atlantic overturning. *Climate Dynamics*, (0123456789). https://doi.org/10.1007/s00382-022-06459-y
Li, F., Lozier, M. S., Holliday, N. P., Johns, W. E., Le Bras, I. A., Moat, B. I., et al. (2021a). Observation-based estimates of heat and freshwater exchanges from the subtropical North Atlantic to the Arctic. *Progress in Oceanography*, *197*(July), 102640. https://doi.org/10.1016/j.pocean.2021.102640
Li, F., Lozier, M. S., Bacon, S., Bower, A. S., Cunningham, S. A., de Jong, M. F., et al. (2021b). Subpolar North Atlantic western boundary density anomalies and the Meridional Overturning Circulation. *Nature Communications*, *12*(1), 1–9. https://doi.org/10.1038/s41467-021-23350-2
Li, Feili, Lozier, M. S., & Johns, W. E. (2017). Calculating the meridional volume, heat, and freshwater transports from an observing system in the subpolar North Atlantic: Observing system simulation experiment. *Journal of Atmospheric and Oceanic Technology*, *34*(7), 1483–1500. https://doi.org/10.1175/JTECH-D-16-0247.1
Lozier, M. S., Li, F., Bacon, S., Bahr, F., Bower, A. S., Cunningham, S. A., et al. (2019). A sea change in our view of overturning in the subpolar North Atlantic. *Science*, *363*(6426), 516–521. https://doi.org/10.1126/science.aau6592
McCartney, M. S., & Talley, L. D. (1982). The Subpolar Mode Water of the North Atlantic. *Journal of Physical Oceanography*, *12*, 1169–1188.
Menary, M. B., Jackson, L. C., &Lozier, M. S. (2020). Reconciling therelationship between the AMOC andLabrador Sea in OSNAP observationsand climate models.*Geophysical Research Letters*,47, e2020GL089793. https://doi.org/10.1029/2020GL089793
Molinari, R. L., Fine, R. A., Wilson, W. D., Curry, R. G., Abell, J., & McCartney, M. S. (1998). The arrival of recently formed Labrador sea water in the Deep Western Boundary Current at 26.5°N. *Geophysical Research Letters*, *25*(13), 2249–2252. https://doi.org/10.1029/98GL01853
Petit, T., Lozier, M. S., Josey, S. A., & Cunningham, S. A. (2020). Atlantic Deep Water Formation Occurs Primarily in the Iceland Basin and Irminger Sea by Local Buoyancy Forcing. *Geophysical Research Letters*, *47*(22), 1–9. https://doi.org/10.1029/2020GL091028
Pickart, R. S., Straneo, F., & Moore, G. W. K. (2003). Is Labrador Sea Water formed in the Irminger basin? *Deep-Sea Research Part I: Oceanographic Research Papers*, *50*(1), 23–52. https://doi.org/10.1016/S0967-0637(02)00134-6
Rhein, M., Fischer, J., Smethie, W. M., Smythe-Wright, D., Weiss, R. F., Mertens, C., et al.

(2002). Labrador Sea Water: Pathways, CFC Inventory, and Formation Rates. *Journal of Physical Oceanography*, *32*(2), 648–665. https://doi.org/10.1175/1520-0485(2002)032<0648:LSWPCI>2.0.CO;2

Rühs, S., Oliver, E. C. J., Biastoch, A., Böning, C. W., Dowd, M., Getzlaff, K., et al. (2021). Changing Spatial Patterns of Deep Convection in the Subpolar North Atlantic. *Journal of Geophysical Research: Oceans*, *126*(7), 1–24. https://doi.org/10.1029/2021JC017245

van Sebille, E., Griffies, S. M., Abernathey, R., Adams, T. P., Berloff, P., Biastoch, A., et al. (2018). Lagrangian ocean analysis: Fundamentals and practices. *Ocean Modelling*, *121*(October 2017), 49–75. https://doi.org/10.1016/j.ocemod.2017.11.008

Van Sebille, E., Baringer, M. O., Johns, W. E., Meinen, C. S., Beal, L. M., De Jong, M. F., & Van Aken, H. M. (2011). Propagation pathways of classical Labrador Sea water from its source region to 26°N. *Journal of Geophysical Research: Oceans*, *116*(12), 1–18. https://doi.org/10.1029/2011JC007171

Spall, M. A., 2004: Boundary Currents and Watermass Transformation in Marginal Seas. *J. Phys. Oceanogr.*, 34, 1197–1213, https://doi.org/10.1175/15200485(2004)034<1197:BCAWTI>2.0.CO;2

Straneo, F., 2006: On the Connection between Dense Water Formation, Overturning, and Poleward Heat Transport in a Convective Basin. *J. Phys. Oceanogr.*, 36, 1822–1840, https://doi.org/10.1175/JPO2932.1

Straneo, F., Pickart, R. S., & Lavender, K. (2003). Spreading of Labrador sea water: An advective-diffusive study based on Lagrangian data. *Deep-Sea Research Part I: Oceanographic Research Papers*, *50*(6), 701–719. https://doi.org/10.1016/S0967-0637(03)00057-8

Susan Lozier, M., Bower, A. S., Furey, H. H., Drouin, K. L., Xu, X., & Zou, S. (2022). Overflow Water Pathways in the North Atlantic. *Progress in Oceanography*, *208*(June), 102874. https://doi.org/10.1016/j.pocean.2022.102874

Thomas, M. D., Tréguier, A.-M., Blanke, B., Deshayes, J., & Voldoire, A. (2015). A Lagrangian Method to Isolate the Impacts of Mixed Layer Subduction on the Meridional Overturning Circulation in a Numerical Model. *Journal of Climate*, *28*(19), 7503–7517. https://doi.org/10.1175/JCLI-D-14-00631.1

Tooth, O. J., Johnson, H. L., & Wilson, C. (2022). Lagrangian Overturning Pathways in the Eastern Subpolar North Atlantic. *Journal of Climate*, (2019), 1–53. https://doi.org/10.1175/jcli-d-21-0985.1

Tsujino, H., Urakawa, L. S., Griffies, S. M., Danabasoglu, G., Adcroft, A. J., Amaral, A. E., et al. (2020). Evaluation of global ocean–sea-ice model simulations based on the experimental protocols of the Ocean Model Intercomparison Project phase 2 (OMIP-2). *Geoscientific Model Development*, *13*(8), 3643–3708. https://doi.org/10.5194/gmd-13-3643-2020

Yashayaev, I., & Loder, J. W. (2016). Recurrent replenishment of Labrador Sea Water and associated decadal-scale variability. *Journal of Geophysical Research: Oceans*, *121*(11), 8095–8114. https://doi.org/10.1002/2016JC012046

Yashayaev, I., Bersch, M., & van Aken, H. M. (2007). Spreading of the Labrador Sea Water to the Irminger and Iceland basins. *Geophysical Research Letters*, *34*(10), 1–8. https://doi.org/10.1029/2006GL028999

Yeager, S. G., Castruccio, F., Chang, P., Danabasoglu, G., & Maroon, E. (2021). An Outsized Role for the Labrador Sea in the Multidecadal Variability of the Atlantic Overturning Circulation. *Science Advances [PREPRINT]*, (October), 1–25.

Zhai, Y., Yang, J., Wan, X., & Zou, S. (2021). The Eastern Atlantic Basin Pathway for the Export of the North Atlantic Deep Waters. *Geophysical Research Letters*, *48*(24), 1–10. https://doi.org/10.1029/2021GL095615

Zou, S., Lozier, M. S., Li, F., Abernathey, R., & Jackson, L. (2020a). Density-compensated overturning in the Labrador Sea. *Nature Geoscience*, *13*(2), 121–126. https://doi.org/10.1038/s41561-019-0517-1

Zou, S., Bower, A., Furey, H., Susan Lozier, M., & Xu, X. (2020b). Redrawing the Iceland−Scotland Overflow Water pathways in the North Atlantic. *Nature Communications*, *11*(1). https://doi.org/10.1038/s41467-020-15513-4